Optimization of Processing Time, Temperature, and Stirring Rate to Synthesize the Ag Nanoparticles Using Oregano Extract

Ahmadi, Omid
Faculty of Chemical Engineering, Sahand University of Technology, Tabriz, I.R. IRAN

Sayyar, Zahra*[+]
Department of Chemical Engineering, University of Bonab, Bonab, I.R. IRAN

Jafarizadeh Malmiri, Hoda
Faculty of Chemical Engineering, Sahand University of Technology, Tabriz, I.R. IRAN

ABSTRACT: *The plant-based extract can be used to synthesize silver nanoparticles (Ag NPs) as a reducing agent. In the present study, Oregano leaves' extracts were extracted using ethanol to synthesize Ag NPs. The effects of different parameters such as the processing time, temperature, and stirring rate on the mean particle size, concentration, and zeta potential of the synthesized Ag NPs solutions were optimized using Response Surface Methodology (RSM). At the optimum condition, which includes processing time (30.48 min), temperature (70 ºC), and stirring rate (370.530 RPM), Ag NPs were obtained with 33 nm of the mean particle size, 76.109 ppm of concentration, and +17.2 mV of zeta-potential. In this condition, Ag NPs displayed high antibacterial activity against Gram-negative and Gram-positive bacteria. In addition, the maximum antioxidant activity of 11.7% was obtained at optimum synthesizing conditions.*

KEYWORDS: *Green synthesis; Silver nanoparticles; Oregano extract; Response Surface Methodology (RSM); Optimization; Antibacterial activity.*

INTRODUCTION

Recently, the synthesis and application of nanoparticles have increased enormously. Unique properties of nanoparticles such as their small size (1-100 nm), physico-chemical, and electronic properties make them different from those of bulk materials [1, 2]. Generally, metal nanoparticles have a high surface area, which make them appropriate for acting as antibacterial and antifungal agent. Because nanoscale improves the electron transfer between valence and conduction bands, therefore metal nanoparticles can be used in different areas as biosensors, biofiltration, drug delivery, antigen delivery for immunization purposes, and bactericides [3-5].

**To whom correspondence should be addressed.*
+ E-mail: z_sayyar@ubonab.ac.ir ; z_sayyar@sut.ac.ir
1021-9986/2023/10/3235-3248 14/$/6.04

In recent years, Ag NPs have attracted much attention due to their unique physical, chemical, biological and applications in various areas such as biomedicine, optoelectronics, optics, catalysis, sensors, etc. Ag NPs can be used in biomedical applications, water and air purification, food production, cosmetics, clothing, and numerous household products due to the broad-spectrum antimicrobial and antifungal properties of silver. Recently, Ag NPs of various sizes and morphologies have been synthesized by using different plant extracts [6-9]. Overall, green nano-biotechnology means synthesizing nanoparticles using biological methods such as those involving microorganisms, plants, and viruses or their by-products, such as proteins and lipids, with the help of various biotechnological tools [10]. Green synthesis methods have several advantages compared to using chemical reagents for synthesizing metal nanoparticles because of rapid and eco-friendly biosynthesis [11-13]. Nanoparticles synthesized using the green method are far superior to those manufactured with physical and chemical methods based on various aspects. For example, green techniques eliminate the use of expensive chemicals, consume less energy, and generate environmentally benign products and by-products [10]. Oregano is from Origanum vulgare L., family Lamiaceae. Oregano Herb is used to treat cough, sore throats and relieve digestive complaints. The extraction of oregano has different antimicrobial and antioxidant activities. Thus ethanolic Oregano leaves' extracts can show high potential to synthesize because of high amount of a reduction agent [14, 15]. Compared to other nanoparticle synthesis methods, using the Bain Mari method can strongly increase reducing agent due to be slow and continuous nucleation. In addition to, heating time, temperature and the stirring rate are three important parameters in Bain Mari technique which can widely change the nucleation and growth of nanoparticles [16]. *Ghaemi et al*. [17] synthesized Ag NPs using algal extract solution. They investigated the effects of numerous parameters such as pH, temperature, the concentration of metal ions and alga, the volume ratio of silver nitrate solution to alga extract, reaction time, mixing order, and the mixing rate of the silver nitrate and the alga extract on the AgNPs synthesis. Their results show that the suitable choice of the reagent ratio, synthesis temperature, pH, concentration of reactants, mixing rate, and mixing order makes it possible to obtain the small particle size. However, synthesizing Ag nanoparticles (Ag NPs) using Oregano extract and an experimental design technique has not been conducted. Oregano extract, as a natural reducing, antioxidant and antimicrobial agents, has been used in various pharmaceutical formulations. Green synthesis of Ag NPs using Oregano extract, results a colloidal solution having both Oregano extract and Ag NPs, which that can be used in numerous pharmaceutical and medicine areas without serious concerns related to the residual of the chemical reagents which those are used commonly in the synthesis of metal NPs and those are toxin for the human and the environment. Furthermore, resulted colloidal solution can be used as new generation of antibiotics which most of the microorganisms, due to the presence of Ag NPs, cannot be resistance against that. Several parameters have influenced the yield of Ag NPs biosynthesis process and the characteristics of the fabricated NPs, in in vitro studies. Operation conditions e.g., heating time, temperature and the stirring rate are the main affecting parameters in the synthesis of inorganic NPs. Therefore, the objective of this study was to synthesize Ag NPs using Oregano extract as a reduction agent. This was obtained using experimental design and statistical analysis with response surface methodology (RSM) which is a set of statistical and mathematical methods to find optimum conditions of factors for desired responses. Therefore, the main objectives of the present paper were (i) to evaluate stable synthesized Ag NPs using Oregano extract; (ii) to optimize parameters (processing time, temperature, and stirring rate) to synthesize Ag NPs with small particle size and high concentration and zeta potential and (iii) to investigate the physico-chemical properties of the obtained Ag NPs (such as the mean particle size, stability, and dispersion of nanoparticles, their antibacterial, and antioxidant activities).

EXPERIMENTAL SECTION

Materials

Oregano was collected from Tabriz, Iran. $AgNO_3$, ethanol (99.8%), and Methanol (99.8%) were bought from Merck Company (Darmstadt, Germany). 2,2-diphenyl-2-picrylhydrazyl (DPPH) was provided from Sigma Aldrich (Louis, Missouri, USA). Deionized double distilled water was applied. *Escherichia coli* (PTCC 1270) and *Staphylococcus aureus* (PTCC 1112) were purchased from microbial Persian-Type Culture Collection (PTCC,

Tehran, Iran). Nutrient Agar (NA) and Potato Dextrose Agar (PDA) were prepared by Biolife Company (Milan, Italy).

Oregano extract prepared

One of the key parts of this study is the extraction of active components of Oregano. Dried and fragmented leaves of Oregano (10 mg) were added to 200 mL of ethanol (30%). Then the solution was put in a Bain Marie at a temperature of 40 ºC for 24 hours. Afterward, Whatman No. 40 filter paper was used to filtrate this mixture. A rotary evaporator was used to remove the residual alcohol from the extraction and it was store at 4 ˚C [9].

Synthesize of Ag NPs

According to the best knowledge, 15 mL of $AgNO_3$ (1 mM) was mixed with Oregano extract (5 mL). Then, Ag NPs were synthesized using the conventional heating method. In this method, the mixture was stirred and heated at different temperatures of 40-80 ºC and 100-400 RPM for 15-75 minutes [18]. Heating time and temperature, and stirring rate are the main physical parameters which those have key effects on reduction of metal ions, converting those to the nanoparticles and increasing the size of the nanoparticles. Therefore, among all chemical and physical parameters, these three factors were selected.

Methods

The concentration of the Ag NPs synthesized was determined by UV–visible spectroscopy measurements (250–800 nm, PERKN ELMER Germany). The size and distribution of the Ag nanoparticles were studied by transmission electron microscopy (TEM, CM120, Philips, Amsterdam, Netherlands). The structural features of Ag nanoparticles was distinguished by X-Ray Diffractometry (XRD: D5000, Siemens Co. Germany) using Cu Kα radiation. Moreover, particle size, polydispersity index (PDI), and zeta potential values were measured using a dynamic light scattering (DLS) particle size analyzer (Nanotrac Wave, Microtrac Inc., Montgomeryville, PA, USA).

Antioxidant assay

To determine the scavenging capability of DPPH, the synthesized Ag NPs (100 µL) were added in 5 mL of methanol (50%) and DPPH radicals (1 mM). Pure DPPH solution was added to the methanol (in a ratio of 1:1) to prepare the control sample. The solutions were stirred in the dark at 27 ˚C for 30 minutes. Lastly, the absorbance maximum of the solutions and blank was noted at 517 nm. Eq. 1 displays the scavenging capability of samples:

$$I\% = (A_{Control} - A_{Sample}) / A_{Control} \times 100 \quad (1)$$

Where $I\%$, $A_{control}$ and A_{sample} represent the inhibition percent, the absorbance of the control, and the absorbance of the samples, respectively [19].

Antimicrobial activity

Antibacterial activity and antifungal activity are both tried for antimicrobial activity. An appropriate diffusion approach based on the stated methodology according to our previous work [20] was used to investigate the antibacterial activity of Ag NPs against both Gram-positive (*S. aureus*) and Gram-negative (*E. coli*) bacteria strains. Briefly, 0.1 mL of the given bacterial suspensions were inoculated on PCA (Plate Count Agar) culture media at the plates, and then 10 µL of the produced samples were put into the inoculated culture media via holes. Finally, the plates were placed in an incubator set at 37 °C for 24 h. The antibacterial activity of the samples was shown by creating a clean zone around the holes. Moreover, the antifungal assay of the samples was done using a method based on the inhibition growth of *Aspergillus flavus* (*A. flavus*) on the PDA (Potato Dextrose Agar) culture media incorporated with Ag NPs. Finally, the plates were put in an incubator at 27°C for five days.

Experimental design

This section is related to the design of the impact of numerous variables with a limited number of experiments to define and clarify the information variation which is assumed to reproduce the variation. A significant influence of variables will be known using statistical analysis of results [21, 22]. A Central Composite Design (CCD) and RSM were applied to predict a quadratic model as a functional relationship between the independent variables and response values. RSM creates many appreciated data by a small number of testing runs to achieve an appropriate model [23, 24]. Furthermore, the impact of three independent factors, i.e., processing time (X_1), temperature (X_2), and stirring rate (RPM: Revolutions per minute) (X_3), on the synthesized Ag NPs was evaluated using RSM. The studied response variables were

Table 1: Experimental runs according to the central composite design and response variables for synthesized Ag NPs

	Temperature of Heater (°C)	Stirring rate (rpm)	Processing time (min)	Concentration (ppm)		Mean Particle size (nm)		Zeta Potential (mV)	
				Experimental	Predicted	Experimental	Predicted	Experimental	Predicted
1	60	250	45	49.35	49.177	50	49.82	16.1	16.09
2	40	250	45	36.74	36.695	74	71.15	14.3	14.55
3	60	100	45	45.58	48.428	62	60.84	13.6	13.92
4	72	160	27	58.99	57.555	49	51.96	14.5	14.24
5	60	250	45	49.78	49.177	49	49.82	16.0	16.09
6	60	400	45	61.43	63.354	47	45.75	16.3	16.66
7	72	340	27	73.74	76.706	39	39.99	17.0	16.42
8	60	250	45	48.90	49.177	51	49.82	16.2	16.09
9	60	250	45	48.81	49.177	50	49.82	16.1	16.09
10	48	340	27	46.25	45.449	64	65.86	14.6	14.32
11	48	340	63	48.35	49.593	57	57.84	15.7	15.46
12	72	340	63	72.53	70.825	44	40.47	16.9	16.97
13	80	160	45	46.36	49.176	47	45.45	16.1	16.43
14	48	160	27	39.78	38.293	55	55.34	12.9	12.44
15	48	160	63	44.78	47.616	69	66.82	14.3	14.38
16	72	160	63	60.25	62.853	56	57.94	15.8	15.83
17	60	250	75	57.36	57.961	47	49.94	15.9	15.83
18	60	250	45	49.68	49.177	49	49.82	16.1	16.09
19	60	250	45	50.02	49.177	49	49.82	16.2	16.09
20	60	250	15	43.53	41.703	66	64.65	13.0	13.75

the concentration (Y_1, ppm), mean Particle size (Y_2, nm), and zeta potential (Y_3, mV) of the synthesized Ag NPs. Based on the literatures, the defined ranges were selected [25-28] and experimental treatments are listed in Table 1. For the center point, 5 repetitions were used to estimate the test error, and an un-coded system was also used to design the experiment by the Minitab software (v.16 statistical package, Minitab Inc., PA, USA). The advantage of repetitions is getting a definite and reasonable result in the test. All tests were done during a day and one block to improve the key independent factors [23, 29].

A second-order polynomial equation was applied (Eq. (2)) to show a relationship between the concentration (Y_1, ppm), mean Particle size (Y_2, nm), and zeta potential (Y_3, mV) of the Ag NPs.

$$Y = \beta_0 + \beta_1 X_1 + \beta_2 X_2 + \beta_3 X_3 + \beta_{11} X_1^2 + \beta_{22} X_2^2 + \beta_{33} X_3^2 + \beta_{12} X_1 X_2 + \beta_{13} X_1 X_3 + |\beta_{23} X_2 X_3 \quad (2)$$

Where β_0, β_i, β_{ii}, and β_{ij} show a constant, the linear, quadratic, and interaction influence, respectively. The determination coefficient (R^2) and adjusted determination coefficient (R^2-adj) were studied to create a proper model to predict. The significance determinations of the obtained models in terms of the p-value (smaller than 0.05) and F ratio (High values) as statistically significant were investigated by analysis of variance (ANOVA). In order to predict the independent variable interactions, three-dimensional surface plots and two-dimensional contour plots were designed on the base of Eq. 2.

Optimization

RSM is a suitable method to evaluate the relationships between the studied responses and experimental data and optimize them to achieve the desired characteristics of the product, because it can generate lots of information from a few experiments and can evaluate the interaction effect between variables on the response [23, 24]. To gain optimum conditions for the independent factors, the obtained surface plots with limitations on the responses of a minimum content for the mean Particle size, as well as a maximum content of the concentration, and zeta potential of the synthesized Ag NPs were estimated. Eventually,

Table 2: Regression coefficients and R^2 of the regression coefficients in the obtained models

	Concentration (ppm)	Mean Particle Size (nm)	Zeta Potential (mV)
	Y_1	Y_2	Y_3
β_0 (constant)	8.967	9.631	6.180
β_1 (main effect)	2.136	1.266	-3.186
β_2 (main effect)	11.643	12.643	8.983
β_3 (main effect)	-1.363	-4.783	2.031
β_{11} (quadratic effect)	0.525	1.924	1.065
β_{22} (quadratic effect)	-1.531	-2.578	-2.610
β_{33} (quadratic effect)	0.021	0.892	1.731
β_{12} (interaction effect)	-0.268	-1.042	-1.473
β_{13} (interaction effect)	0.514	0.952	1.601
β_{23} (interaction effect)	1.614	2.833	2.931
R^2	%95.99	%96.42	%97.21

Table 3. P-value of the regression coefficients in the obtained models

		Concentration (ppm)	Mean Particle Size (nm)	Zeta Potential (mV)
		Y_1	Y_2	Y_3
		p-value		
Main	X_1	0.039	0.047	0.010
	X_2	0.002	0.001	0.004
	X_3	0.014	0.028	0.031
Quadratic	X_1^2	0.103	0.127	0.044
	X_2^2	0.038	0.028	0.036
	X_3^2	0.045	0.046	0.012
Interaction	X_1X_2	0.156	0.160	0.291
	X_1X_3	0.212	0.374	0.187
	X_2X_3	0.042	0.021	0.233

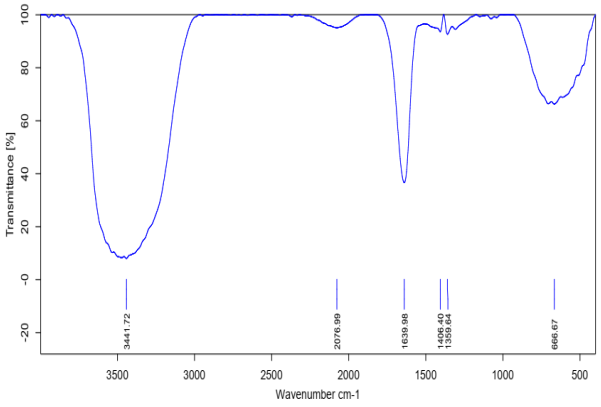

Fig. 1: FT-IR spectrum of oregano extract

three extra approval tests were carried out at the optimal point to verify the validity of the experimental data.

RESULTS AND DISCUSSIONS

Fourier transform-infrared (FT-IR) spectra analysis

In order to identify the possible reducing and stabilizing biomolecules of Oregano extract, FT-IR measurements were carried out. The FT-IR spectra of Oregano extract were recorded using KBr pellets in the 4000–400 cm^{-1} region. The FT-IR spectrum of Oregano extract is shown in Fig. 1. The absorption peak centered at 3441.72 cm^{-1} referred to the O-H (hydroxyl groups) responsible for reducing the Ag^+ ions to atoms (Ag^0) and stabilizing agents of the leaf extract (monoterpenes and sesquiterpenes) in the silver NPs synthesis. Moreover, absorption peak at 1639.98 cm^{-1} stretching vibration of C=C (alkane and amide I groups), are responsible for stabilizing the NPs.

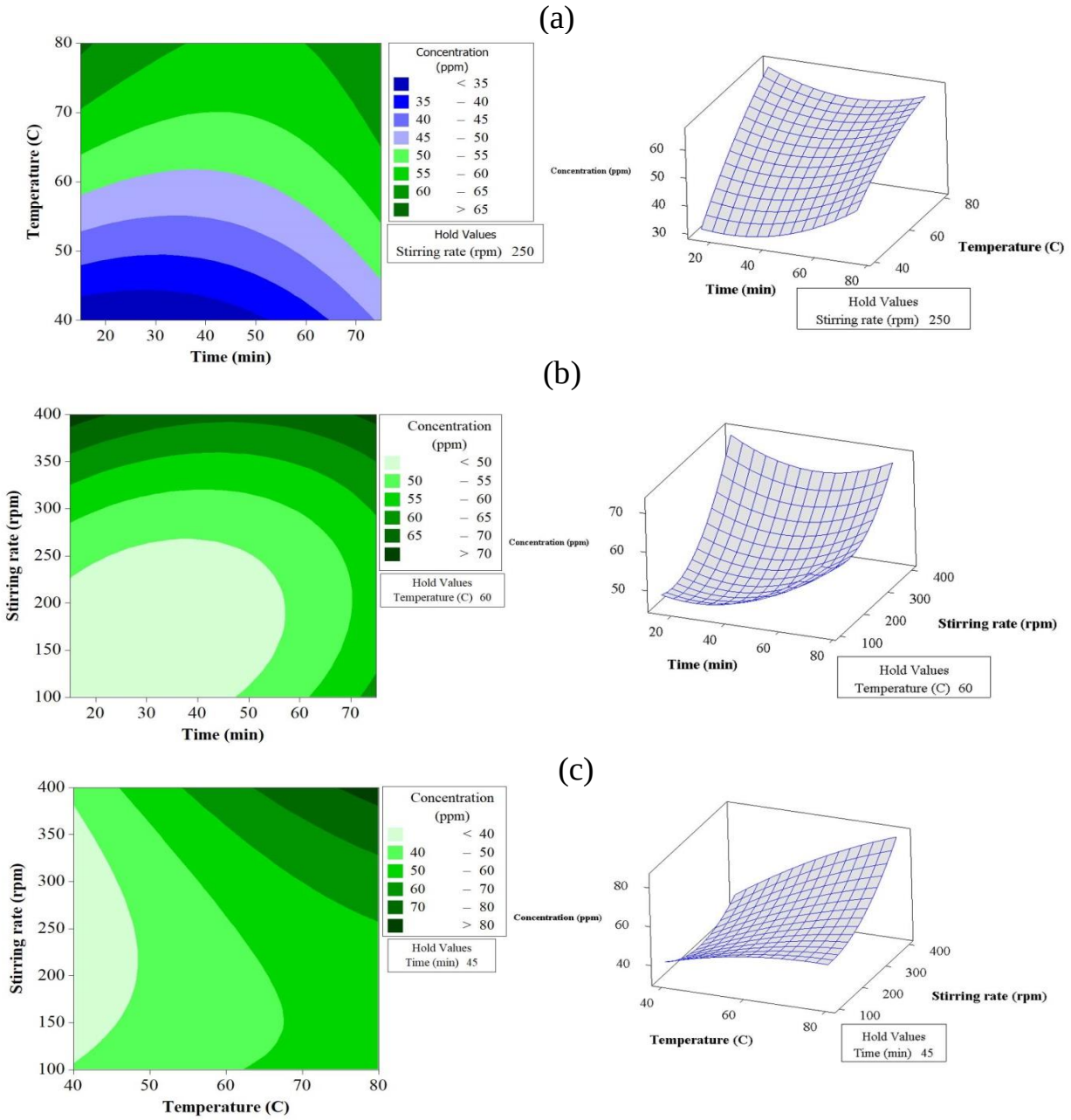

Fig. 2. Response surface and contour plots for the concentration of Ag nanoparticles as a function of significant interaction effects of a) temperature and time, b) the stirring rate and time, and c) the stirring rate and temperature

Fitting the Response Surface Models (RSM)

Second-order polynomial models and multiple regression analysis were applied to study three parameters for Ag NPs synthesis in Table 1. Also, Table 2 shows the predictable coefficients of regression and the corresponding significance of regressions for the second-order polynomial models.

Also, all parameters such as p-values of all the main, quadratic, and interaction terms of the achieved models are given in Table 3. Typically, high values of the R^2 for these models showed a high accuracy of the models and their good performance.

According to Table 2, the effect of variables is important, and it can be concluded that the independent variables impact on the dependent variables because of $p<0.05$ and the main terms of the synthesis variables played a key role to achieve all responses.

The Effects of parameters on the concentration of Ag NPs

One of the main aim of this project is to synthesize Ag NPs with a high concentration. UV analysis may be used to predict the concentration of Ag NPs. In fact, the concentration of Ag NPs is calculated using the calibration curve. The concentration of Ag NPs is given in Table 1. The effects of temperature and time of the synthesis process at a constant stirring rate (250 RPM) on the concentration of the synthesized Ag NPs are shown in Fig. 2a. In the low processing time, the concentration of synthesized nanoparticles increased with the increase in temperature, and this trend is also observed in the high time of the synthesis process. Moreover, at low and constant temperatures of the process, the concentration of Ag NPs increased by increasing the time of the synthesis process, while at constant and high temperatures of the process, this trend is not observed.

It seems that comparing the effects of temperature with the time of the synthesis process, the temperature variable has a greater effect. Therefore, at the appropriate temperature, the reaction between silver metal ions and reducing agents will take place and nanoparticles will be synthesized.

Fig. 2b displays the effects of stirring rate and processing time at the constant temperature on the concentration of synthesized Ag NPs.

As shown in Fig. 2b, at the constant and low time, the concentration of nanoparticles increased continuously by increasing the stirring rate; meanwhile, at the constant and high time of the synthesis process, this trend has relatively reduced. Also, at low and constant values of the stirring rate, the concentration of synthesized Ag NPs increased continuously by increasing in the time of the process, but at high and constant values of the stirring rate, this trend was almost constant and increasing the processing time had no effect on the concentration of synthesized Ag NPs. It seems that the reaction between reducing agents and silver nitrate salt does not take place completely at the low processing time and stirring rate. Therefore, the presence of substances that have not yet been converted into nanoparticles and act as disturbing factors in the reaction. These reasons can be the cause of the low concentration of synthesized Ag NPs.

The effects of process temperature and the stirring rate at a constant processing time on the concentration of the synthesized Ag NPs are presented in Fig. 2c.

According to this Fig., at a constant and low process temperature, significant changes are not observed in the concentration of Ag NPs by increasing the stirring rate, but this trend is completely opposite at a high process temperature, so the concentration of Ag NPs increase by increasing the stirring rate. At constant and low values of the stirring rate, the concentration of the synthesized Ag NPs has increased slightly by increasing temperature such that these changes at a high and constant stirring rate increase significantly by increasing temperature. Based on mentioned points, there must be a proper balance between the parameters and the silver nitrate salt to obtain proper concentration. At low temperatures, the reaction probability is low, and the reaction between reducing agents and silver metal ions will be carried out for long periods of time. Increasing the string rate will not affect the concentration of nanoparticles, but at high process temperature, the molecules are constantly moving and the probability of collision and reaction is high; therefore, these collisions naturally increase and the probability of the reaction and production of silver nanoparticles will increase by increasing stirring rate. The low reaction temperature significantly slowed down the generation of nuclei and growth, therefore, it took a longer time to complete the reduction of precursors and increase the concentration of synthesized Ag nanoparticles. The reaction rate increased with rising temperature and processing time, as well as the concentration of synthesized Ag nanoparticles.

The Effects of temperature, time and constant stirring rate of the synthesis process on the particles size of Ag NPs

The effects of temperature and time of the synthesis process at a constant stirring rate (250 RPM) on the particle size of Ag NPs are shown in Fig. 3a.

According to the result, at low and constant processing time, the mean particle size of the synthesized Ag NPs decreased by increasing process temperature; meanwhile, this trend is also observed at high and constant processing time. At low and constant process temperature, the mean particle size of Ag NPs has decreased by increasing the processing time, but at high and constant process temperatures, a completely double behavior is observed by increasing the processing time. It seems that the Ag NPs collide with each other due to high molecular dynamics therefore, the average size of the particles increased.

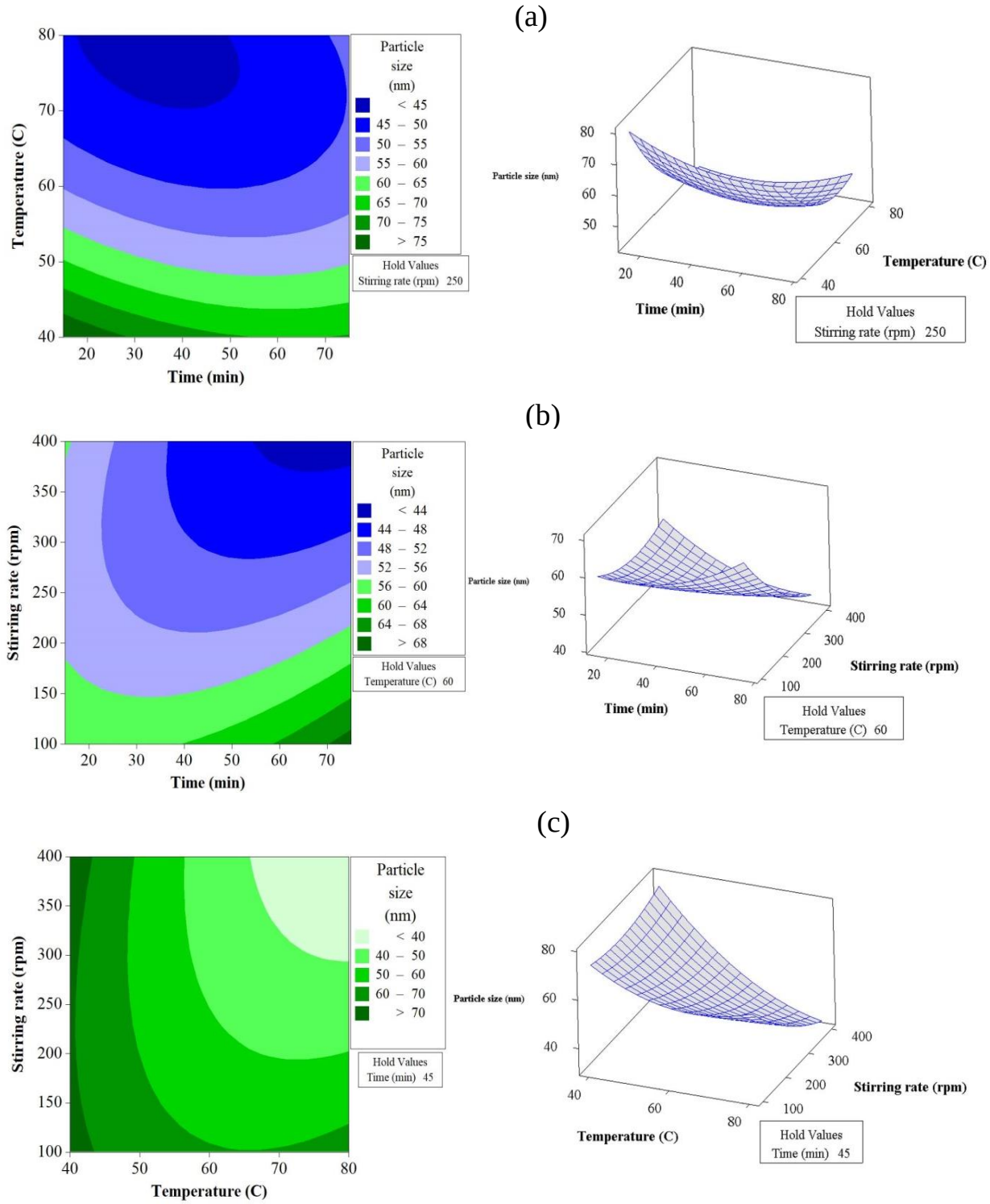

Fig. 3: Response surface and contour plots for the mean particle size of Ag nanoparticles as a function of significant interaction effects of a) temperature and time, b) the stirring rate and time, and c) the stirring rate and temperature

Fig. 3b displays the effects of stirring rate and processing time at the constant temperature on the particle size of Ag NPs. By comparing the effects of parameters, at low and constant processing time, no significant changes

in the mean particle size of Ag NPs were observed by increasing the stirring rate, but at constant and high processing time. Furthermore, increasing the stirring rate has a high effect on the mean particle size. At low and constant values of the stirring rate, a relative increase in the mean particle size of the synthesized nanoparticles is observed by increasing processing time, and this trend is completely opposite at the high and constant stirring speed by increasing the processing time. At a low stirring rate, there is no proper mixing between reducing agents and silver nitrate metal salt, therefore, increasing the processing time acts as a completely inappropriate factor to obtain a high mean particle size.

The effects of process temperature and the stirring rate at a constant processing time on the particle size of Ag NPs are presented in Fig. 3c.

At a constant and low reaction temperature, increasing the stirring rate did not affect the mean particle size of Ag NPs and showed an almost constant trend, but at a high process temperature, increasing the stirring rate had a completely positive effect. It seems that increasing the two factors of the process temperature and stirring rate has positive effects on Ag NPs. By a large increasing temperature, nanoparticles can become agglomerated, which is an undesirable phenomenon in the synthesis of nanoparticles, and finally, the size of nanoparticles will increase as these particles stick together. Also, by raising in the processing time, they have in the direction of synergy with the temperature due to the unfavorable effect. Therefore, they will cause the production of nanoparticles with a larger size. Consequently, the high and suitable temperature prevents the increase of particle size and finally the produced nanoparticles will have good quality and low mean particle size. In the other hand, by increasing the hearing time, the moving speed of the formed Ag NPs in the solution was enhanced, which in turn, increased the collision frequency between NPs increased and resulted in their decreased particle size.

The Effects of parameters on the zeta-potential of Ag NPs

The effects of temperature and time of the synthesis process at a constant stirring rate (250 RPM) on the zeta-potential of Ag NPs are shown in Fig. 4a. At constant and low or high temperatures, zeta-potential increased by increasing time. The long processing time in the synthesis process of Ag NPs is an inappropriate factor to reduce the surface charge and ultimately reduce the repulsive power of the synthesized particles, and finally, the nanoparticles will lose their stability. Moreover, at low processing time and temperature, plant regenerating substances have not yet found enough opportunity and energy to reduce silver nitrate metallic salt, and therefore the zeta-potential of Ag NPs was low. Fig. 4b displays the effects of stirring rate and processing time at the constant temperature on the zeta-potential of Ag NPs. At the constant and low stirring rates, increasing the processing time has a high effect on the zeta-potential of the Ag NPs. Also, increasing stirring rate had a great effect on the zeta-potential. It seems that, at a high the stirring rate, the Ag NPs have sufficient physical stability. The effects of process temperature and the stirring rate at a constant processing time on the zeta-potential of Ag NPs are presented in Fig. 4c.

At constant low or a high values of the stirring rates, the zeta potential has increased by increasing the process temperature, and this increase is more evident at high stirring rate and vice versa. At high the process temperature, increasing zeta potential is more visible. The zeta potential of the synthesized Ag NPs showed that the presence of opposite charges around these nanoparticles has not undergone adverse changes with the increase in processing time, temperature, and stringing rate. It seems that one of the most effective factors in creating surface charges in synthesized silver nanoparticles is the selection of appropriate agents.

Optimization

To obtain the smallest particle size and the highest concentration and Zeta-potential for synthesized Ag NPs, the optimization of conditions should be done. Therefore, graphical optimization was plotted to detect the best condition for the parameters. The desired processing time, temperature, and stirring rate were achieved to obtain the optimum particle size, concentration, and Zeta-potential. Numerical multiple optimization was also applied to obtain the exact optimal values of the studied synthesis variables. The results of numerical optimization indicated that the synthesis of Ag nanoparticles was obtained at the optimal point, which includes the processing time of 30.48 min, the process temperature of 70 ºC, and the stirring rate of 370.530 RPM. Experimental showed that the mean particle size, concentration, and Zeta-potential of Ag NPs were equal to 31.27 nm, 76.50 ppm, and +17.55 mV,

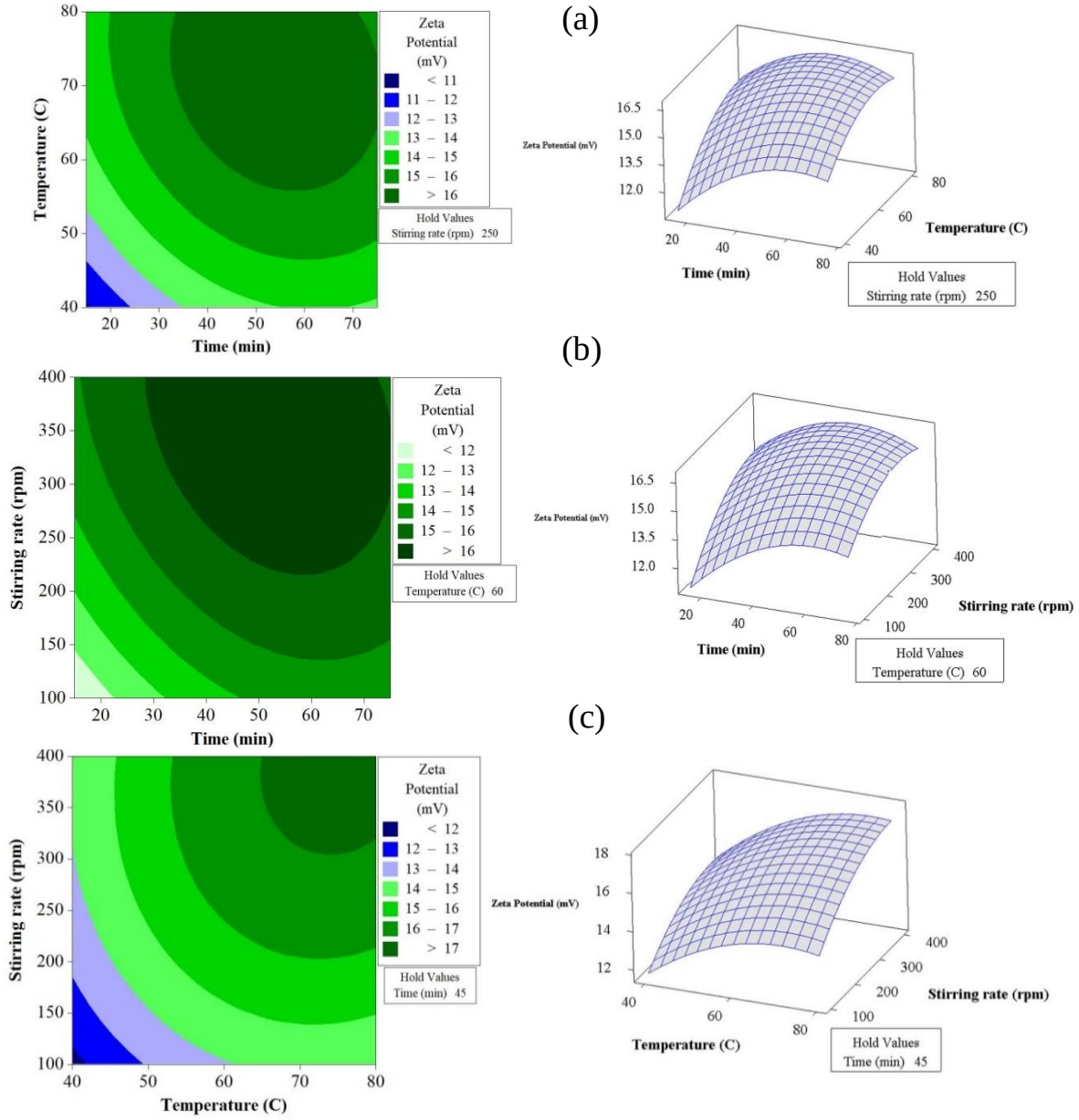

Fig. 4: Response surface and contour plots for the zeta-potential of Ag nanoparticles as a function of significant interaction effects of a) temperature and time, b) the stirring rate and time, and c) the stirring rate and temperature

respectively. However, *Ghanbari et al*. [13] synthesized silver nanoparticles (AgNPs) using Aspergillus fumigatus (A. fumigatus) mycelia extract via the hydrothermal method. Mean particle size, polydispersity index (PDI) value, and maximum ζ potential value of 23 nm, 0.270, and +35.3 mV, respectively, were obtained.

The concentration of synthesized Ag NPs

Moreover, three Ag NPs solutions were synthesized based on the suggested optimal values by numerical multiple optimizations and characterized in terms of studied response variables. The synthesis of Ag NPs from the 1 mM solution of $AgNO_3$ in the presence of Oregano extract was established by using UV-Vis spectral analysis (Fig. 5a). At the optimum conditions, Ag NPs were synthesized with a concentration of 76.109 ppm. The insignificant differences between the anticipated and the experimental data at obtained optimal conditions demonstrated the suitability of the fitted models for considered responses. By optimizing the parameters, it seems that

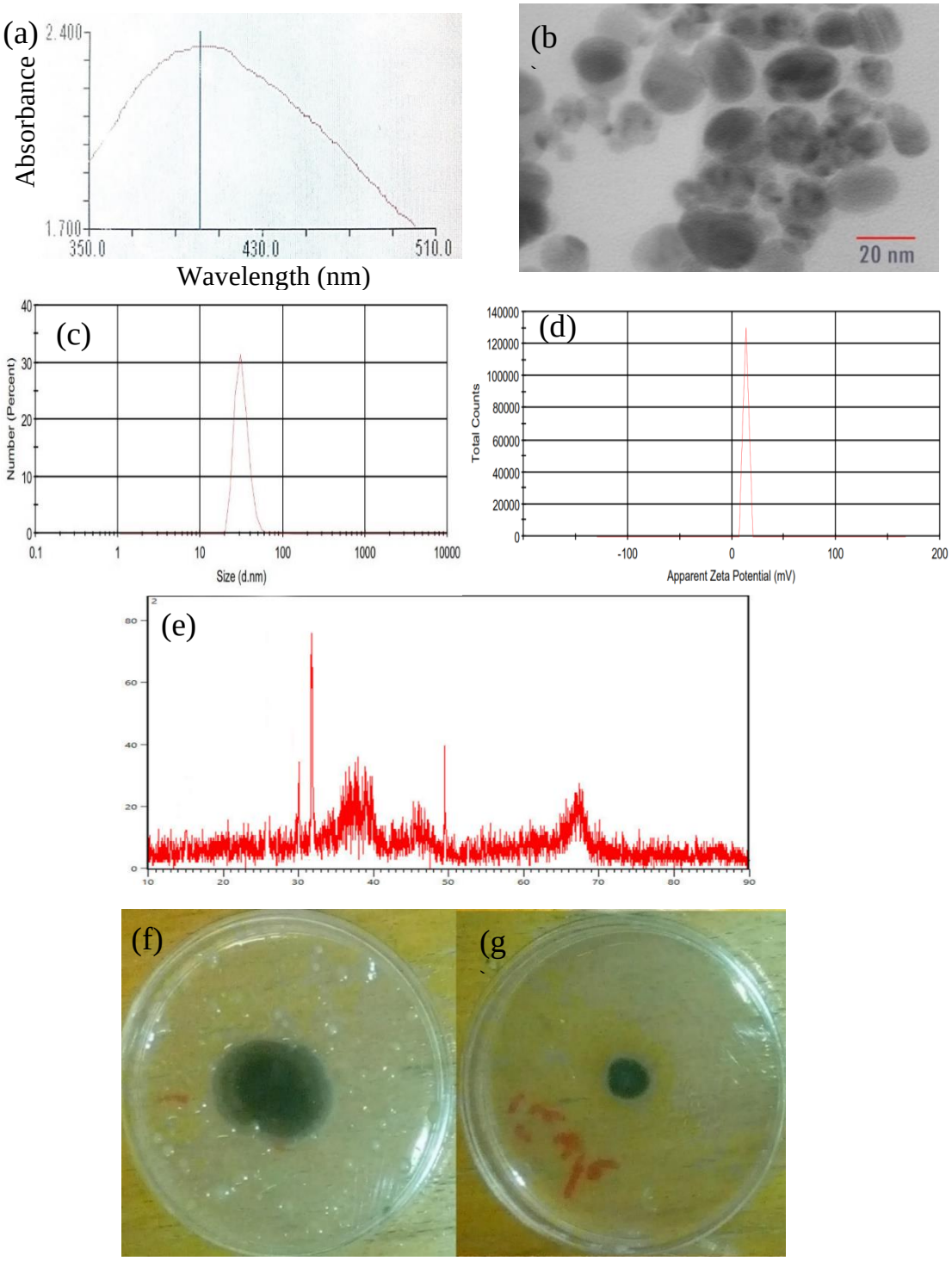

Fig. 5: a) UV-Vis analysis, b) TEM image, c) mean particle size, d) zeta-potential, e) XRD analysis, g) antifungal of the synthesized Ag nanoparticles at optimum conditions, and f) control fungal

the temperature, stirring rate and processing time obtained have a suitable effect on the concentration of synthesized Ag nanoparticles, and this effect has caused the production of nanoparticles with suitable properties.

The morphology

In this section, TEM analysis was used to scan synthesized nanoparticles at the optimum point. Fig. 5b exhibits a TEM micrograph of the morphology of the

synthesized Ag NPs. As shown, the synthesized Ag NPs had a spherical shape and good distribution; therefore, they presented good stability.

The particle size and zeta-potential

The particle size and zeta-potential of the synthesized Ag NPs were measured at 25 ºC using DLS (Nanotrac Wave, Microtrac, USA). The size distributions and zeta-potential of synthesized Ag NPs at obtained optimum conditions are also presented in Fig. 5c and d. The measured experimental values for the mean particle size and zeta-potential of the synthesized Ag NPs were 33 nm and +17.2 mV, respectively. The insignificant differences found between the predicted values and the experimental values of the optimum suggested a sample that was reconfirmed by the adequacy of the fitted models for studied responses.

XRD analysis

Figure 5e shows X-ray diffractometer of the crystalline nature of Ag NPs by the (Fig 5e). The peaks of silver at 2θ around 32°, 38°, 44°, and 68° are related to the (101), (111), (200), and (220) sets of lattice planes of the face-centered cubic structure of silver and its crystalline nature. The comparison was performed between the XRD patterns in this study and the pure crystalline silver structure present in Joint Committee on Powder Diffraction Standards (JCPDS) file, which corresponds to no. 04-0783.

Antioxidant assay

The percentage of antioxidant activity of the synthesized silver nanoparticles at optimum operation conditions was evaluated. The results showed that Ag NPs had a potent antioxidant activity with 11.7% inhibitory properties. In order to compare the antioxidant properties of nanoparticles with Oregano extract and silver salt solution, the antioxidant analysis showed that the antioxidant of the extract and silver nitrate were 2.4 and 1.7%, respectively. It is concluded that the high antioxidant property of Ag NPs is due to their nanostructure.

Antimicrobial activity

The antibacterial activity of the synthesized Ag NPs was estimated against both Gram-negative and Gram-positive bacteria. In order to compare the antioxidant properties of nanoparticles with Oregano extract and silver salt solution, the antibacterial activity showed that the antibacterial of the synthesized Ag NPs, silver nitrate solution, and Oregano extract were 3.4, 1, and 0.6 cm, against Gram-positive bacteria and 2.7, 0.9, and 0.6 cm against Gram-negative bacteria, respectively. The achieved results can be explained by the fact that Ag NPs have the potential to kill the cells by entering the bacterial cell wall. These results showed the generation of Reactive Oxygen Species (ROS) that happened using Ag NPs. The Ag NPs exhibited the highest ROS generation in the bacteria cells. The highest generation of ROS might be the reason for the highest ability of Ag NPs to produce antibacterial activity. Furthermore, Fig. 5f shows inhibition of the *A. flavus* mycelia growth against Ag NPs compared to the control plates in Fig. 5g. The results exhibited that the synthesized Ag NPs have higher antifungal activity.

CONCLUSIONS

The silver nanoparticles were synthesized using a conventional heating and Oregano extract (as both reducing and stabilizing agents). To the best of our knowledge, this technique has not been previously described in the works. According to the results, RSM was suitable for studying the impact of the synthesis factors on the dependent variables. Furthermore, optimization of factors was done to get the most desirable Ag NPs. At the optimum conditions, Ag NPs were synthesized with a concentration of 76.109 ppm. The TEM analysis exhibited the morphology of the synthesized Ag NPs with small particle sizes and narrow size distribution. Oregano extract and silver salt solution, the antioxidant analysis showed that the antioxidant of the extract and silver nitrate were 2.4 and 1.7%, respectively. Finally, Ag NPs had a high antioxidant activity with 11.7% inhibitory properties, and then the antibacterial activity rate of Ag NPs was more than 3.4 cm against Gram-positive bacteria.

Received : Dec.15, 2022 ; Accepted : May. 22, 2023

REFERENCES

[1] Yousaf S., Chopra H., Khan M.A., Mustafa F., Kamal, M.A., and Baig A.A., Nanotechnology and Its Applications: Insight into Bacteriological Interactions and Bacterial Gene Transfer, *Micro- Nanotechnol. Biomed*, 479-497 (2022).

[2] De Marchi L., Coppola F., Soares A.M., Pretti C., Monserrat J.M., Della Torre C., Freitas R., Engineered Nanomaterials: From their Properties and Applications, to their Toxicity Towards Marine Bivalves in a Changing Environment, *Environ. Res*., **178**: 108683 (2019).

[3] Rana A., Yadav K., Jagadevan., A Comprehensive Review on Green Synthesis of Nature-Inspired Metal Nanoparticles: Mechanism, Application and Toxicity, *J. Cleaner Prod*., **272**: 122880 (2020).

[4] Bhalla N., Jayaprakash A., Ingle N., Patel H., Srilakshmi P.V., Haranath D., Fabrication and Infusion of Potent Silver Doped Nano ZnO Aimed to Advance Germicidal Efficacy of Health and Hygiene Products, *J. Sci.: Adv. Mater. Devices*, 100487, (2022).

[5] Pathania D., Kumar S., Thakur P., Chaudhary V., Kaushik A., Varma R.S., Furukawa H., Sharma M., Khosla A., Essential Oil-Mediated Biocompatible Magnesium Nanoparticles with Enhanced Antibacterial, Antifungal, and Photocatalytic Efficacies, *Sci. Rep.*, **12(1)**: 1-13 (2022).

[6] Ahmadi O., Jafarizadeh-Malmiri H., Jodeiri N.J.G.P., Synthesis. Eco-friendly Microwave-Enhanced Green Synthesis of Silver Nanoparticles Using Aloe Vera Leaf Extract and their Physico-Chemical and Antibacterial Studies, *Green Process. Synth*., **7(3)**: 231-240 (2018).

[7] Ahmadi O., Jafarizadeh-Malmiri H., Jodeiri N., Optimization of Processing Parameters for Hydrothermal Silver Nanoparticles Synthesis Using Aloe Vera Leaf Extract and Estimation of their Physico-Chemical and Antifungal Properties, *Z. Phys. Chem.*, **233(5)**: 651-667 (2019).

[8] Ahmadi O., Jafarizadeh-Malmiri H. Biotechnology. Green Approach in Food Nanotechnology Based on Subcritical Water: Effects of Thyme Oil and Saponin on Characteristics of the Prepared Oil in Water Nanoemulsions, *Food Sci. Biotech*., **29(6)**: 783-792 (2020).

[9] Mohammadlou M., Jafarizadeh-Malmiri H., and Maghsoudi H., Hydrothermal Green Synthesis of Silver Nanoparticles Using Pelargonium/Geranium Leaf Extract and Evaluation of their Antifungal Activity, *Green Process. Synth.*, **6 (1)**: 31-42 (2017).

[10] Parveen K., Banse V., Ledwani L., Green Synthesis of Nanoparticles: Their Advantages and Disadvantages, *AIP Conference Proceedings*, **1724(1)**: 020048 (2016).

[11] Jafarizadeh-Malmiri H., Anarjan N., Berenjian A., Developing three-Component Ginger-Cinnamon-Cardamom Composite Essential Oil Nanoemulsion as Natural Food preservatives, *Environ. Res*., **204**: 112133 (2022).

[12] Scandorieiro S. et al., Synergistic and Additive Effect of Oregano Essential Oil and Biological SILVER NAnoparticles AGAINST MULTIDRuG-ResistanT Bacterial STRains, *Front. Microbiol*., **7**: 760 (2016).

[13] Ghanbari S., Vaghari H., Sayyar Z., Adibpour M., Jafarizadeh-Malmiri H., Autoclave-Assisted Green Synthesis of Silver Nanoparticles Using A. Fumigatus Mycelia Extract and the Evaluation of Aheir Physico-Chemical Properties and Antibacterial Activity, *Green Process. Synth*., **7(3)**: 217-224 (2018).

[14] MeretoudiA., Banti C.N., Raptis P.K., Papachristodoulou C., Kourkoumelis N., Ikiades A.A., Zoumpoulakis P., Mavromoustakos T., Hadjikakou S.K., Silver Nanoparticles from Oregano Leaves' Extracts as Antimicrobial Components for Non-Infected Hydrogel Contact Lenses, *Int. J. Mole. Sci.*, **22(7)**: 3539 (2021).

[15] Ahmed A., Talaat I., Khalid K., Soil Moisture and Glutamic Acid Affect Yield, Volatile Oil and Proline Contents of Oregano Herb (Origanum Vulgare L.), *Int. J. Botany*, **13(1)**: 43-51 (2017).

[16] Howes P.D., Chandrawati R., Stevens M.M., Colloidal Nanoparticles as Advanced Biological Sensors, *Sci*., **346(6205)**: 1247390 (2014).

[17] Ghaemi M. Gholamipoor S., Controllable Synthesis and Characterization of Silver Nanoparticles using Sargassum Angotifolium (2017).

[18] Eshghi M., Kamali-Shojaei A., Vaghari H., Najian Y., Mohebian Z., Ahmadi O., Jafarizadeh-Malmiri H., Synthesis. Corylus Avellana Leaf Extract-Mediated Green Synthesis of Antifungal Silver Nanoparticles Using Microwave Irradiation and Assessment of Their Properties, *Green Process. Synth.*, **10 (1)**: 606-613, (2021).

[19] Shah B.R., Zhang C., Li Y., Li B., Bioaccessibility and Antioxidant Activity of Curcumin after Encapsulated by Nano and Pickering Emulsion Based on Chitosan-Tripolyphosphate Nanoparticles, *Food Res. Int*., **89**: 399-407 (2016).

[20] Sayyar Z., Jafarizadeh-Malmiri H., Beheshtizadeh N., A Study on the Anticancer and Antimicrobial Activity of Curcumin Nanodispersion and Synthesized ZnO nanoparticles, *Process Biochem*., **121**: 18-25 (2022).

[21] Sharma N., Mishra S., Sharma S., Deshpande R.D., Sharma R.K., Preparation and Optimization of Nanoemulsions for targeting Drug Delivery, *Int. J. Drug Dev. Res*., **5(4)**: 0975-9344 (2013).

[22] Gutiérrez J., González C., Maestro A., Sole I., Pey C., Nolla J., Nano-emulsions: New Applications and Optimization of Their Preparation, *Curr. Opin. Colloid Interface Sci*., **13(4)**: 245-251 (2008).

[23] Anarjan N., Jaberi N., Yeganeh-Zare S., Banafshehchin E., Rahimirad A., Jafarizadeh-Malmiri H., Optimization of Mixing Parameters for α-Tocopherol Nanodispersions Prepared Using Solvent Displacement Method, *J. Am. Oil Chem. Soc*., **91(8)**: 1397-1405 (2014).

[24] Galooyak S.S., Dabir B., Three-Factor Response Surface Optimization of Nano-Emulsion Formation Using a Microfluidizer, *J. Food Sci. Technol.*, **52(5)**: 2558-2571 (2015).

[25] Alahmad A., Al-Zereini W.A., Hijazin T.J., Al-Madanat O.Y., Alghoraibi I., Al-Qaralleh O., Al-Qaraleh S., Feldhoff A., Walter J-G., Scheper T., Green Synthesis of Silver Nanoparticles Using Hypericum perforatum L. Aqueous Extract with the Evaluation of Its Antibacterial Activity Against Clinical and Food Pathogens. *Pharmaceutics*, **14(5)**: 1104 (2022).

[26] Jafari A., Vaghari H. Jafarizadeh-Malmiri H., Development of Antimicrobial Films Based on Aloe vera and Fabricated AgNPs Using Propolis, *Proc. Natl. Acad. Sci., India, Sect. B Biol. Sci*., **91**: 95–103 (2021).

[27] L. Shastri H. N. Abdelhamid M. Nawaz H.-F. Wu, Synthesis, Characterization and Bifunctional Applications of Bidentate Silver Nanoparticle Assisted Single drop Microextraction as a Highly Sensitive Preconcentrating Probe for Protein Analysis, *RSC Advances*, **5(52)**: 41595-41603 (2015).

[28] Tippayawat P., Phromviyo N., Boueroy P., Chomposor A., Green Synthesis of Silver Nanoparticles in Aloe Vera Plant Extract Prepared by a Hydrothermal Method and Tanaheir Synergistic Antibacterial Activity, *Peer J*., **4(29)**: 2589 (2016).

[29] Bezerra M.A., Santelli R.E., Oliveira E.P., Villar L.S., Escaleira L.A., Response Surface Methodology (RSM) as a Tool for Optimization in Analytical Chemistry, *Talanta*, **76(5)**: 965-977, (2008).